Received: 14 January 2018 | Revised: 17 August 2018 | Accepted: 22 August 2018

DOI: 10.1111/gbi.12315

ORIGINAL ARTICLE

WILEY gebiology

The Sirius Passet Lagerstätte of North Greenland—A geochemical window on early Cambrian low-oxygen environments and ecosystems

Emma U. Hammarlund[1,2] | M. Paul Smith[3] | Jan A. Rasmussen[4] | Arne T. Nielsen[5] | Donald E. Canfield[1] | David A. T. Harper[6]

[1]Nordic Center for Earth Evolution, Institute of Biology, University of Southern Denmark, Odense M, Denmark

[2]Department of Laboratory Medicine, Translational Cancer Research, Lund University, Lund, Sweden

[3]Oxford University Museum of Natural History, Oxford, UK

[4]Fossil and Moclay Museum, Museum Mors, Nykøbing Mors, Denmark

[5]Department and Geoscience and Natural Resources, Copenhagen University, Copenhagen K, Denmark

[6]Palaeoecosystems Group, Department of Earth Sciences, Durham University, Durham, UK

Correspondence
Emma U. Hammarlund, Nordic Center for Earth Evolution, Institute of Biology, University of Southern Denmark, Odense M, Denmark.
Email: emma@biology.sdu.dk

Funding information
Villum Fonden, Grant/Award Number: 16518; Geocenter Danmark; Danmarks Grundforskningsfond, Grant/Award Number: DNRF53; Wenner-Gren Foundation; Agouron Institute; Carlsbergfondet; Leverhulme Trust; The Swedish Research Council

Abstract

The early Cambrian Sirius Passet fauna of northernmost Greenland (Cambrian Series 2, Stage 3) contains exceptionally preserved soft tissues that provide an important window to early animal evolution, while the surrounding sediment holds critical data on the palaeodepositional water-column chemistry. The present study combines palaeontological data with a multiproxy geochemical approach based on samples collected in situ at high stratigraphic resolution from Sirius Passet. After careful consideration of chemical alterations during burial, our results demonstrate that fossil preservation and biodiversity show significant correlation with iron enrichments (Fe_{HR}/Fe_T), trace metal behaviour (V/Al), and changes in nitrogen cycling ($\delta^{15}N$). These data, together with Mo/Al and the preservation of organic carbon (TOC), are consistent with a water column that was transiently low in oxygen concentration, or even intermittently anoxic. When compared with the biogeochemical characteristics of modern oxygen minimum zones (OMZs), geochemical and palaeontological data collectively suggest that oxygen concentrations as low as 0.2–0.4 ml/L restricted bioturbation but not the development of a largely nektobenthic community of predators and scavengers. We envisage for the Sirius Passet biota a depositional setting where anoxic water column conditions developed and passed over the depositional site, possibly in association with sea-level change, and where this early Cambrian biota was established in conditions with very low oxygen.

KEYWORDS
Cambrian explosion, geochemistry, oxygen minimum zone, Sirius Passet, soft-tissue fossil preservation, water-column chemistry

1 | INTRODUCTION

Our understanding of the early diversification of animals is largely based on the exceptional preservation of soft-tissue faunas preserved in lower Palaeozoic Lagerstätten deposits (Conway Morris, 1989; Knoll & Carroll, 1999). Conditions promoting soft-tissue preservation were particularly common during the early and middle Cambrian Period (Cambrian series 2 and 3), when, for example, the renowned

Burgess Shale-type (BST) preservation mode involved carbonaceous impressions (Gaines, 2014). Of the exceptionally preserved biotas of the early Cambrian Period, the Sirius Passet fossil assemblage in North Greenland is the most geographically remote and the least well known.

The Sirius Passet fauna is dominated by soft-bodied arthropods, and only a single species (the trilobite *Buenellus higginsi* Blaker, 1988) had a calcareous exoskeleton (Peel, 2010). The modes of fossil preservation appear variable (Stein, Budd, Peel, & Harper, 2013), and the dominant mode is not definitively established. Some fossils of mainly biomineralized taxa are preserved with three-dimensional (3D) relief, while soft-bodied taxa are preserved as two-dimensional (2D) impressions coated by a reflective and—presumably—organic film (Conway Morris & Peel, 1995; Stein, Peel, Siveter, & Williams, 2010; Topper, Greco, Hofmann, Beeby, & Harper, 2018; Vinther, Smith, & Harper, 2011). Such 2D impressions, particularly if coated by reflective film, associate the Sirius Passet fossils with typical BST preservation (Butterfield, 1995) and, thus, with other BST deposits, such as the Chengjiang deposit of the Yangtze platform in South China and the Burgess Shale of western Canada (Gaines, 2014). The Sirius Passet fauna is apparently of lower diversity than other Cambrian BST Lagerstätten (Gaines, 2014) and distinct through its absence of macro-algae (a feature only shared with the early Cambrian Emu Bay Lagerstätte) (Ivantsov et al., 2005), which presumably reflects a deeper, sub-photic zone setting.

The inferred age of the Sirius Passet biota is based on the presence of the abundant trilobite *Buenellus higginsi*, which most likely correlates the succession with the *Nevadella* trilobite Biozone in Laurentia, equated with Stage 3 of the Cambrian Period (521–514 Ma) (Cohen, Finney, Gibbard, & Fan, 2013). Its age is therefore similar to the Chengjiang Lagerstätte, also determined as Cambrian Series 2 and Stage 3 in age (Gaines, 2014). The Yangtze platform provides most of the current geochemical data on early Cambrian environments, from which both recurrent water-column stratification (Canfield et al., 2008; Cremonese et al., 2013; Feng, Li, Huang, Chang, & Chu, 2014; Hammarlund et al., 2017; Wen, Fan, Zhang, Cloquet, & Carignan, 2015) and oxygenation (Chen et al., 2015) are inferred. For Sirius Passet, interpretations of the palaeodepositional water-column chemistry are few, divergent, and mainly based on macrofossil evidence. For example, the subordinate presence of bioturbation (Ineson & Peel, 2011), a palynology similar to that of other low-oxygen settings (Vidal & Peel, 1993) and the fact that halkieriids (a lophotrochozoan) are preserved somewhat curved, resembling how worms coil up in sudden anoxic conditions (Conway Morris & Peel, 1995), have all been taken to suggest a largely inhospitable water column. Thus, Budd (1995) was the first to acknowledge the challenge of resolving how the soft-tissue Sirius Passet fauna was preserved effectively in situ in an environment that hosted *some* trace makers. Since then, the subordinate presence of bioturbation (here evidenced by laminated mudrock, but see Kristensen et al., 2012, for definitions within bioturbation), in combination with seemingly autochthonous faunal components, has been taken to reflect a habitable setting that resembles the edges of oxygen minimum zones (OMZs) (Budd, 1995; Ineson & Peel, 2011). Finally, a predominantly oxic water column—but with a fluctuating oxycline—was inferred from the absence of iron and molybdenum enrichments that are typical of euxinic settings as reported by Boudec et al. (2014). These authors also discussed a model where the geochemistry could reflect OMZ-like conditions, but reasoned that if such conditions facilitated soft-tissue preservation, both phenomena should be associated throughout the Phanerozoic Eon (Boudec et al., 2014). Since soft-tissue preservation is not generally associated with OMZs in the Phanerozoic, the model invoking OMZ-like conditions was rejected. Taken together, neither the macrofossils nor the chemical signatures from Sirius Passet provide unambiguous clues regarding the depositional conditions. Or conversely, both macrofossils and chemical signatures may reflect an ambiguous depositional setting.

Deciphering water-column chemistry at Sirius Passet must also consider the extent to which geochemical signals reflect metamorphic alteration or the rapid influx of sediments from shallower-water settings. During the Ellesmerian Orogeny in the middle Palaeozoic, iron-rich chloritoid porphyroblasts formed in the Sirius Passet sediments (Ineson & Peel, 2011). This iron-associated alteration of the rocks demands care when applying iron as an indicator of the depositional setting, and we attempt to evaluate how iron was redistributed into silicates during metamorphism (see Methods). With regard to the possible influx of sediments from a shallower-water setting, gravity flows of sediments are a common characteristic in classical BST sites (Gaines, 2014), but have been less clearly visible at Sirius Passet. Indeed, the apparent lack of features representing transport of fossils (Vidal & Peel, 1993) has in part led to the interpretation of Sirius Passet as one of the deepest-water Cambrian Lagerstätten deposits (Ivantsov et al., 2005). Recently, however, lithological observations suggest the presence of sediment gravity flows (e.g., features within the thin laminae, such as grading, scouring and cross-lamination) and for transport of at least some of the Sirius Passet fauna to their site of deposition (Strang, Armstrong, Harper, & Trabucho-Alexandre, 2016). The preservation of large and non-compressed fossils with delicate morphologies at Sirius Passet, such as the 20 cm large arthropod *Arthroaspis* (cf. Budd, 1995; Stein et al., 2013), is difficult to reconcile with transport.

Here, we present high-resolution geochemical, sedimentological and biodiversity data from the Sirius Passet Lagerstätte, sampled in situ in north-western Peary Land in 2011, in which we aim to assess the chemical conditions in the shelf sea inhabited by these animal communities. The geochemical results reflect a low-oxygen setting and show that the Sirius Passet fauna shares characteristics with faunas in the vicinity of modern OMZs.

2 | GEOLOGICAL SETTING

The Sirius Passet fossils are preserved within the mud-dominated "Transitional" Buen Formation (Ineson & Peel, 2011), which

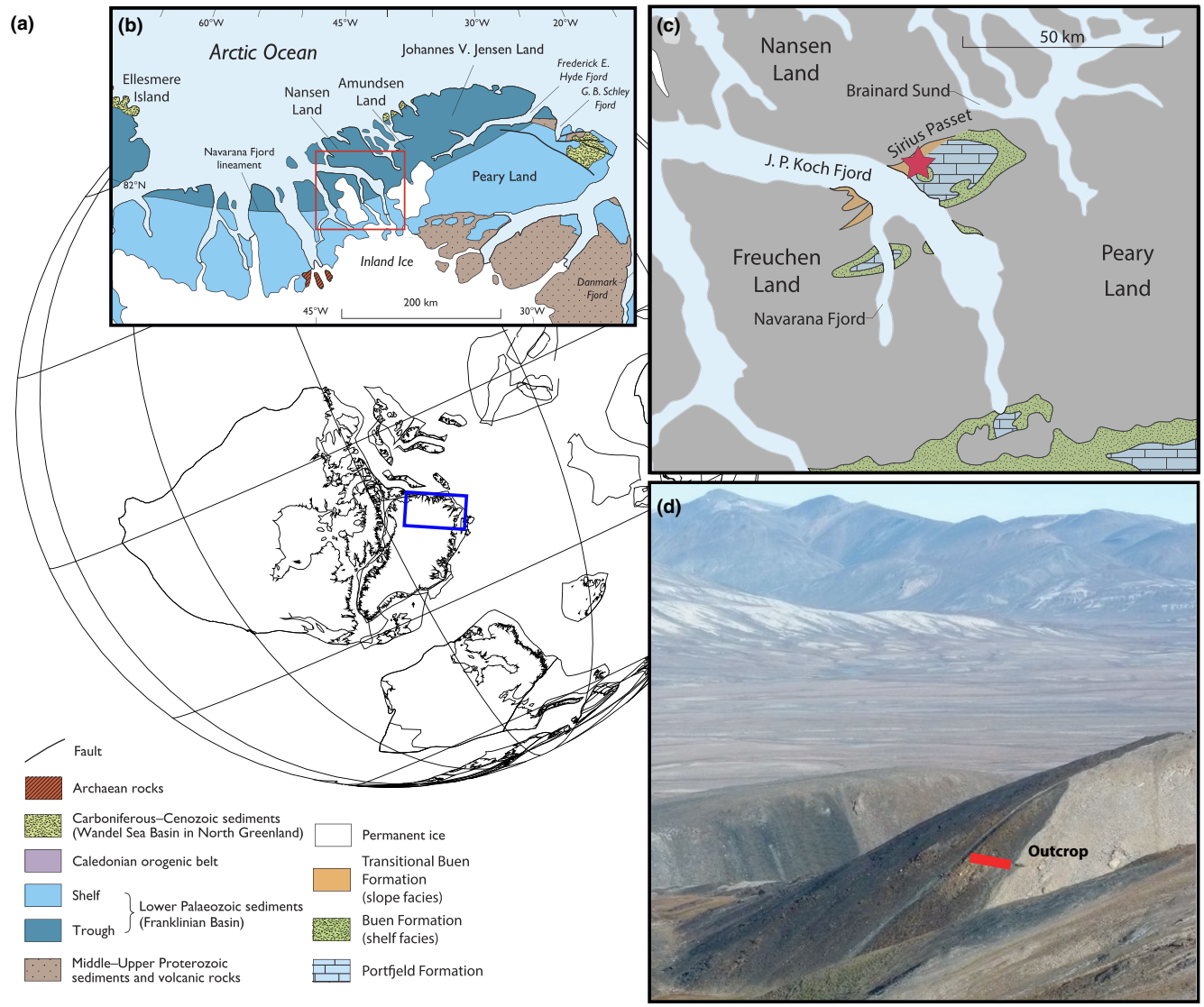

FIGURE 1 The Sirius Passet locality in North Greenland. (a) Location of North Greenland in the early Cambrian at ~520 Ma (Cocks & Torsvik, 2002) constructed in Bugplates (Torsvik, 2009). (b) The eastern Franklinian Basin (modified from Ineson & Peel, 2011). (c) The Sirius Passet locality at 82˚47.59′N 42˚13.54′W, east of JP Koch Fjord is marked with a star (modified from Boudec et al., 2014). (d) The fossiliferous main outcrop (red line) on the west-facing slope at the south-west end of Sirius Passet

was deposited on the continental shelf at low latitudes during Cambrian Series 2, Stage 3 (Figure 1). The shelf was part of the contiguous northern margin of the Laurentian continent, with a stratigraphy that can be traced for several thousand kilometres along strike, from North Greenland into Nunavut, Canada (Higgins, Ineson, Peel, Surlyk, & Sønderholm, 1991). The typical shelf Buen Formation comprises a lower sand-dominated part and an upper mudstone and siltstone-dominated part, reflecting an overall upward deepening trend (Higgins et al., 1991). However, smaller-scale cycles of upward coarsening (shallowing) are also seen within the mud-dominated part (Ineson & Peel, 2011). The Sirius Passet Lagerstätte has been considered by some authors to have been deposited in a slope setting, flanking the margin of a carbonate platform succession of the older Portfjeld Formation (Ineson & Peel, 2011). In this scenario, normal faulting, probably related to uplift of the Portfjeld Formation and degradation of the carbonate platform, resulted in a near vertical contact between the Portfjeld Formation and the outboard "Transitional" Buen Formation (Ineson & Peel, 2011). Degradation of the carbonate platform would then have resulted in megablocks, or olistoliths, breaking off the fault scarp that subsequently were draped by "Transitional" Buen mudstone (Ineson & Peel, 2011).

Fossil occurrences have been noted at six localities within a 1 km section along the carbonate platform margin. The Sirius Passet Lagerstätte is recognized at only one locality, where it occurs within a stratigraphically restricted mudstone succession approximately 12 m thick. Distinct 1–10 mm laminations dominate the fossiliferous interval (Figure 2). Several elements of the Sirius Passet fauna such

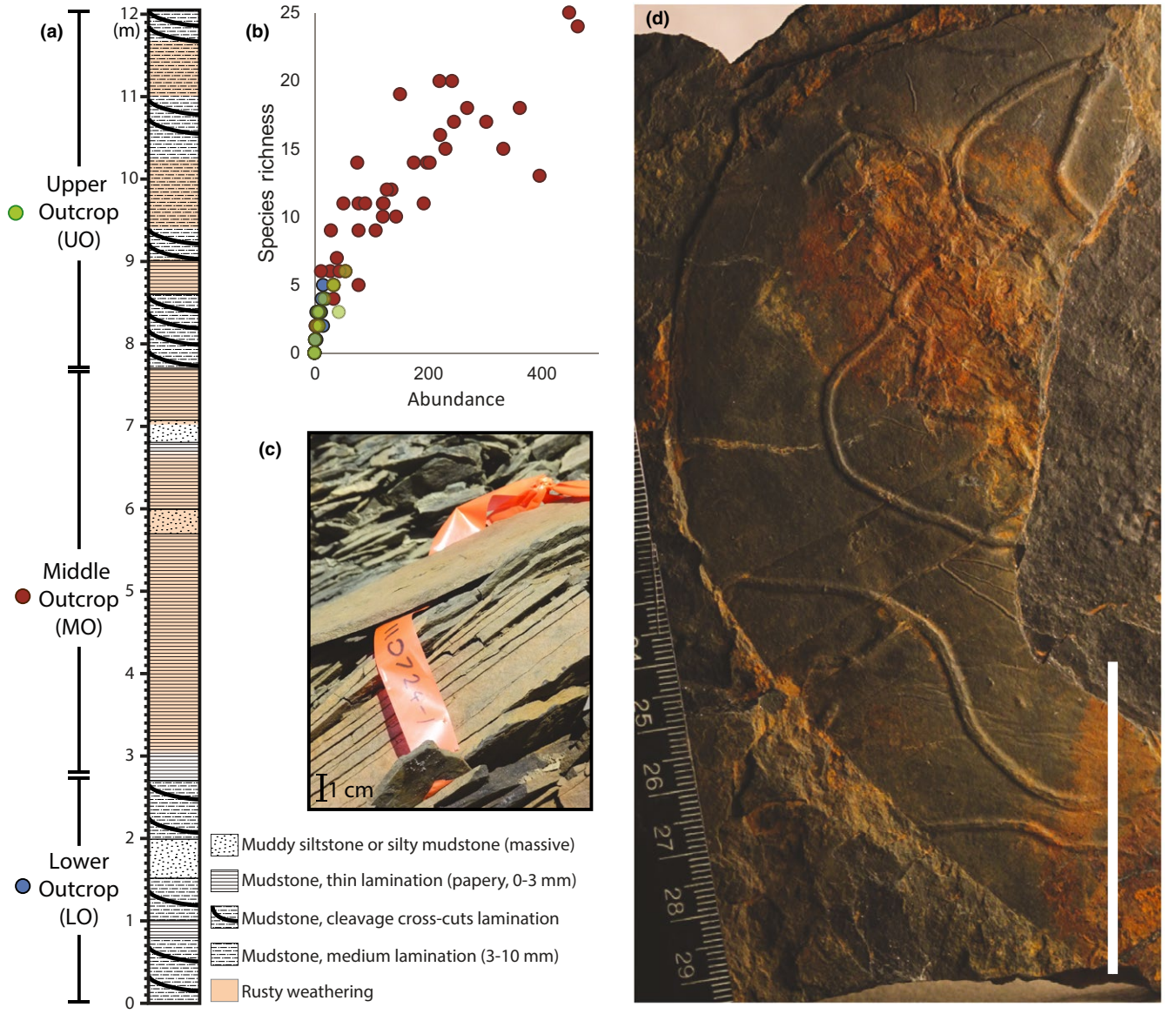

FIGURE 2 (a) The stratigraphic column of the fossiliferous interval. (b) Abundance of fossils vs diversity at the sample levels (sourced from respective interval marked as blue (LO), red (MO) and green (UO). (c) Thinly laminated, rusty, paper shale in the most fossiliferous interval (3–8 m). (d) A slab with a large *Arthroaspis* arthropod, its rusty gut tract and associated trace fossils (cf. Mángano et al., 2012), scale bar (white) 5 cm

as the bivalved arthropod *Isoxys* have a cosmopolitan distribution (Legg & Vannier, 2013) that indicates an active connection to the global ocean. Bioturbation that disrupts sediment lamination has been reported (Ineson & Peel, 2011), and principally occurs above and below the fossiliferous interval. Within the fossiliferous Sirius Passet deposit, small calibre, horizontal burrow systems do occur, with preferential concentration within and adjacent to the decaying arthropod carcasses (Budd, 2011; Mángano et al., 2012). The distinctive network of interconnected and sometimes dendritic burrow system is interpreted to have been constructed by meiofauna and small macrofaunal invertebrates (Mángano et al., 2012), and this burrowing does not disrupt sedimentary lamination. Samples for this study were collected within the fossiliferous interval, primarily from mudstones. The sedimentary facies are consistent with deposition below storm wave base with intermittent, dilute, gravity flow deposits derived from shallower water.

The Buen Formation is exposed sporadically along strike for ~500 km adjacent to the northern margin of the Portfjeld carbonate platform. Deformation of this margin and the northern part of the outcrop belt occurred during the end-Devonian Ellesmerian Orogeny (~345 Ma) (Ineson & Peel, 2011), resulting in thrusting, folding and metamorphism. This Devonian orogenic event is also associated with the generation of abundant chlorite and chloritoid growth in the Sirius Passet mudstones, indicating a greenschist-grade metamorphic overprint (Budd, 1995). The strata at the Lagerstätte locality dip at 48° and sedimentary way-up criteria, comprising graded beds and truncated cross-bedding (Strang, Armstrong, Harper, & Trabucho-Alexandre, 2016), have been

determined throughout the interval of the fossiliferous Transitional Buen Formation. These sedimentary criteria confirmed a structural inversion (Strang, Armstrong, Harper, & Trabucho-Alexandre, 2016) of the Sirius Passet locality (contra Ineson & Peel, 2011) and thus a faulted, rather than stratigraphic, contact with the adjacent carbonates of the Portfjeld Formation.

3 | METHODS

During an expedition to northern Peary Land, northernmost Greenland, in July 2011, the fossiliferous section was measured in situ and extended by careful excavation on the west-facing slope of a hill at the south-western end of the Sirius Passet valley (at 82°47.59′N 42°13.54′W or 23 × 058723 UTM 9195030, 420 m above sea level). Over an interval of 12.2 m, 144 samples were collected for geochemical analysis (average spacing of 8.5 cm). The relative height in the sample suite spans −0.15 to +12.05 m. Fossil abundance was evaluated by splitting the rocks, noting volume of the rock and the number of each species, while the dorso-ventral orientation of the trilobite *Buenellus higginsi* (*n* = 737) was also measured.

Iron (Fe) speciation analyses follow the methodology of Poulton and Canfield (2005), where the residual sediment was subsequently boiled (12N HCl, 1 min) to determine the pool of poorly reactive iron (Fe_{PR})(Raiswell & Canfield, 1998). Gravimetric pyrite estimations follow Canfield (1989, and references therein). These analyses include standard sediments (e.g., NRCC PACS-2 and in-house standards), measured multiple times (STDV < 0.1). To determine contents of organic C (TOC) and total N (TN), inorganic carbon was removed (1N HCl for 2 hr). Isotope analyses of the pyritic sulphur (S), organic carbon and nitrogen (N) were performed by isotope ratio mass spectrometry (Thermo Delta V plus) after combustion in an elemental analyser Flash EA 1112 (S) or Flash EA 2000 (C and N). For calibration of the S isotope measurements, the international standards IAEA S1, S2 and S3 were used. For calibration of N and C isotope determinations, international standards of sediment (IVA 33802151), protein (IVA 33802155) and urea (IVA 33802174) were used. The isotopic composition of pyrite S ($\delta^{34}S_{PY}$) is reported relative to the Vienna Cañon Diablo troilite (V-CDT) with a precision of 0.5 ‰. The isotopic composition of carbon ($\delta^{13}C$) is reported as relative to Vienna Pee Dee Belemnite (V-PDB), with a precision of 0.3 ‰, and the isotopic composition of N ($\delta^{15}N$) is reported relative to air, with a precision of 0.6 ‰. Measurements of C and N concentrations had standard deviations of 0.06 wt% (C) and 0.05 wt% (N).

The elemental compositions of total iron (Fe_T), vanadium (V) and molybdenum (Mo) were measured with a hand-held energy dispersive XRF spectrometer (HHXRF) model Delta DP-6000 with Rh anode from Olympus. The HHXRF was calibrated against split samples in which trace metals contents were separately determined by XRF calibrated against certified standards. The individual elements absorbing X-rays were identified with Olympus Soil and Geochem software, using the Compton model to correct for noise. To perform the HHXRF, rock powder (<63 μm) in vials was covered with thin plastic kitchen wrap and measured up-side-down with 120 s on each of the two beams (see more in Dahl et al., 2013). We determined the concentrations after calibrating the HHXRF data against certified rock standards at an accuracy generally within 10%. Repeated HHXRF determinations of the certified standard NRC PACS-2 yielded standard deviations of the element content of <1% for Fe, 9% for V and 12% for Mo.

4 | RESULTS

4.1 | Lithology and biodiversity

The rock samples (*n* = 144) mainly consist of mudstones with some muddy siltstones at ~6 and ~7 m in the measured section (Figure 2). The fossiliferous mudstones are predominantly laminated, classified here as either thin laminations (2–4 mm or papery) or medium thick laminations (4–10 mm). The main interval of thinly laminated mudstone straddles 2.8–7.7 m. In some intervals, the plane of cleavage cross-cuts lamination (bedding plane). In horizons with thin laminations, the weathered rock colour is rusty (Figure 2c). A clear lithological shift, from the compact mudstone (with silt) to more flaggy (i.e., fissile but cemented enough to be sampled in large slabs) shale, occurs at 1.72 m. We define three intervals within the ~12 m thick main outcrop, based on the interval below, within and above the thinly laminated mudstones (2.8–7.7 m). The intervals are referred to as the lower outcrop (LO) at 0–2.8 m, the middle outcrop (MO) at 2.8–7.7 m and the upper outcrop (UO) at 7.8–12.1 m.

Overall, out of 49 recorded species, 20 were observed only once or twice. The MO is the most fossil rich interval, where the species richness is ~20-fold higher and the abundance ~300-fold higher than in the LO or the UO (Figure 3). The trilobite *Buenellus higginsi* occurs with the convex, dorsal surface up in only 7% of the specimens (*n* = 737), confirming the inversion of the strata noted from sedimentary structures. Less than 1% of the trilobite specimens are disarticulated and fossil disarticulation is noted more commonly in the annelid species. Four nektobenthic taxa, *Buenellus*, *Arthroaspis*, *Campanumuta* and *Kleptothule*, comprise about 30% of the specimens identified (*n* = 6245). The distributions of these four common nektobenthic taxa through the section are indicated on Figure 6, next to that of the nektonic *Isoxys* (Nielsen, Rasmussen, & Harper, 2017; Williams, Siveter, & Peel, 1996), which comprises 55% of the specimens. No evidence of vertically disruptive bioturbation was observed within the succession.

4.2 | Geochemistry of the Sirius Passet Lagerstätte

Geochemical data are presented in Figure 3. The Fe_{HR}/Fe_T ratios are low in the LO (mean 0.10, std ±0.03), higher in the MO (0.23 ± 0.11) and low again in the UO (0.14 ± 0.06). The values within MO occasionally exceed (with maximum of 0.69) the "anoxic threshold" (Fe_{HR}/Fe_T > 0.38) conventionally used to determine anoxic settings Poulton & Canfield, 2011). We tested the relation between

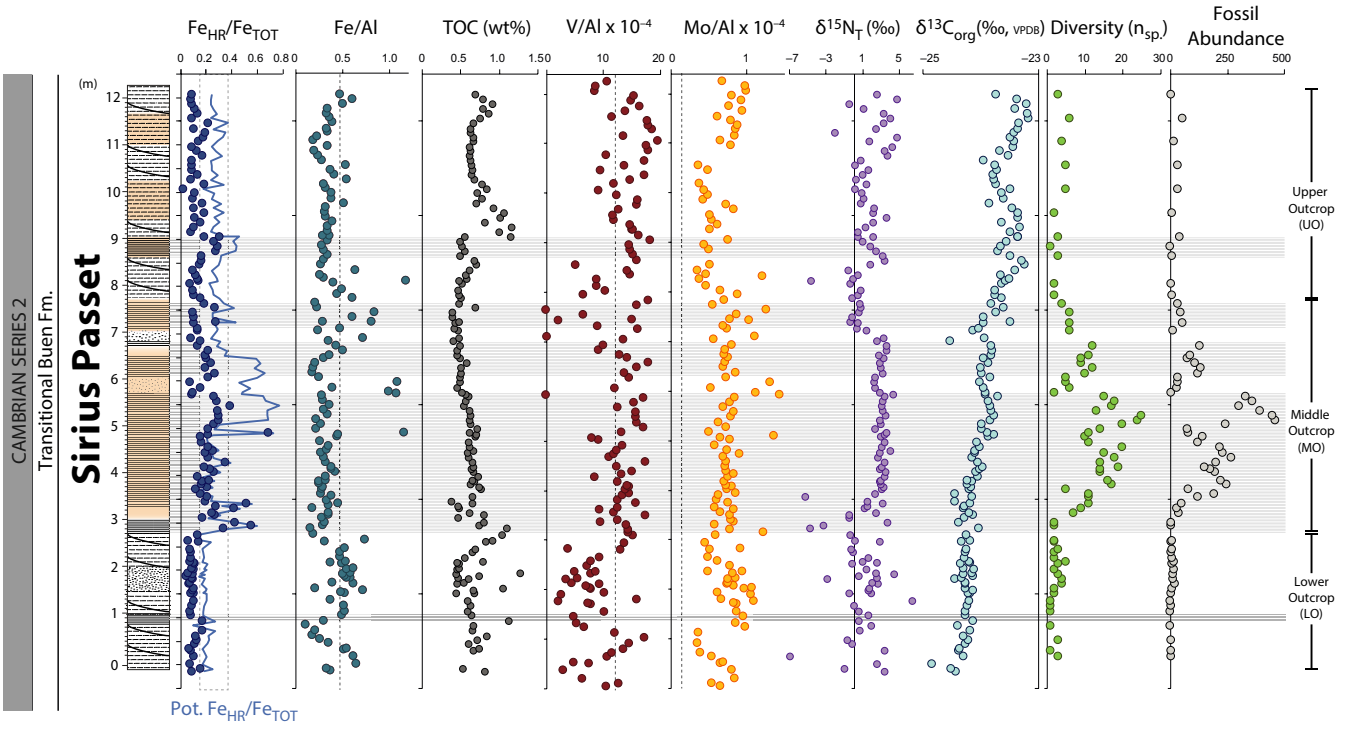

FIGURE 3 Geochemical data from the succession. Fe$_{HR}$/Fe$_T$ (*Potential* Fe$_{HR}$/Fe$_T$ as a blue line; intermediate zone between the Cambrian average (0.14) and the threshold commonly used to distinguish anoxic water-column conditions (0.38) marked with dashed lines (Poulton & Canfield, 2011; Poulton & Raiswell, 2002)), Fe/Al, TOC (wt%), V/Al, Mo/Al (dashed lines mark crustal averages) δ^{15}N$_T$ (‰), δ^{13}C$_{org}$ (‰), diversity (number of species) and abundance (number of fossils found) within the lower (LO), middle (MO) and upper (UO) outcrop intervals

the Fe$_{HR}$/Fe$_T$ data and the "anoxic threshold" by use of the non-parametric Wilcoxon signed-rank test, since Fe$_{HR}$/Fe$_T$ is not normally distributed. The test revealed that the Fe$_{HR}$/Fe$_T$ sample median within the MO is significantly different from 0.38 (that is lower than 0.38). However, the values are significantly higher than average Fe$_{HR}$/Fe$_T$ ratios in Cambrian sediments deposited below presumably oxic water columns (0.14 ± 0.11) (Poulton & Raiswell, 2002) as indicated by the Wilcoxon signed-rank test.

The ratios of Fe$_{HR}$/Fe$_T$ may become altered during metamorphism and diagenesis (Poulton & Canfield, 2011), and at Sirius Passet, the growth of iron-rich chloritoid porphyroblasts likely gathered iron oxides from the pool of highly reactive iron (Fe$_{HR}$). Since iron in chlorite, and in other sheet silicates, is generally not extracted in the Fe$_{HR}$ steps (Poulton & Canfield, 2005; and references herein), such remobilization would alter the proxy of reactive iron so that indications of anoxia are lost. In principle, our data could then underestimate the Fe$_{HR}$/Fe$_T$ at the time of deposition and thus the extent of anoxia. Therefore, we tested the relationship between poorly reactive iron and total iron (Fe$_{PR}$/Fe$_T$) in our dataset with values from other Cambrian rocks. We used the parametric Students t test to test the mean values, since the Fe$_{PR}$/Fe$_T$ data are normally distributed. In support of iron remobilization, we note that the proportion of poorly reactive iron, Fe$_{PR}$/Fe$_T$ (0.53 ± 0.31), particularly in the LO (0.70 ± 0.17), is significantly higher than the average Fe$_{PR}$/Fe$_T$ in lower Cambrian rocks (0.41 ± 0.11, n = 60) (Poulton & Raiswell, 2002) and generally inversely correlated to Fe$_{HR}$/Fe$_T$ (Supporting Information Figure S1). The observation that poorly reactive iron (Fe$_{PR}$) is generally higher in samples with low Fe$_{HR}$/Fe$_T$ (below the Cambrian average of 0.14 (Poulton & Raiswell, 2002), see Supporting Information Figure S1), leads us to conclude that remobilization of highly reactive Fe has occurred.

To attempt an evaluation of reactive iron loss, we calculated a "*Potential* Fe$_{HR}$" and its proportion of Fe$_T$ ("*Potential* Fe$_{HR}$"/Fe$_T$). To estimate the fraction of Fe$_{HR}$ that potentially has been scavenged into Fe$_{PR}$, we set a so-called Fe$_{PR}$ reference line. Although all samples would have been affected by remobilization, or scavenging, of highly reactive Fe, we utilize the fact that samples with high Fe$_{HR}$/Fe$_T$ (above the Cambrian average of 0.14 (Poulton & Raiswell, 2002), see Supporting Information Appendix S1) have significantly less Fe$_{PR}$ (Supporting Information Figure S1). A "Fe$_{PR}$ reference line" is set as the average Fe$_{PR}$ in samples with Fe$_{HR}$/Fe$_T$ above the Cambrian average of 0.14, in each of the intervals (LO, MO and UO). To estimate the relative remobilization, the positive difference between the "reference Fe$_{PR}$" and the Fe$_{PR}$ in each sample is considered to comprise a minimum estimate of scavenged Fe$_{HR}$. When this calculated pool of scavenged Fe$_{HR}$ for each interval (LO, MO, and UO) is added to each sample's Fe$_{HR}$/Fe$_T$, it forms a "*Potential* Fe$_{HR}$/Fe$_T$" (see Supporting Information Figure S2 and Appendix S1 for details). The "*Potential* Fe$_{HR}$/Fe$_T$" is presented (blue line) next to the Fe$_{HR}$/Fe$_T$ ratios in Figure 3.

Although conceptual, this evaluation depicts that—potentially—Fe_{HR}/Fe_T was higher, particularly in the upper MO (0.38 ± 0.17) and in the UO (0.29 ± 0.06) intervals, before metamorphism of the sediments. Thus, indications of anoxia during the deposition of the fossiliferous MO are suggested by, in its lower part, Fe_{HR}/Fe_T values that exceed 0.38, and in its upper part, by *Potential* Fe_{HR}/Fe_T values that exceed 0.38. In the upper part of the MO, furthermore, increasing Fe/Al values (max 1.09), compared to otherwise low and variable values (0.41 ± 0.18) may also reflect anoxic conditions (Lyons & Severmann, 2006). Overall, our effort to evaluate iron remobilization emphasizes an initially ambiguous dataset that requires interpretation utilizing several kinds of observations.

Trace metal enrichments, normalized to the lithogenic background of each element, are utilized here since changes in the nature of the lithogenic flux appear small (as assessed through the Al/Ti which is 23.9 ± 2.0, see Supporting Information Data S1 and Figure S8). Molybdenum contents (Mo/Al) within the outcrop are generally uniform (0.74 ± 0.21) and above the crustal average (0.14) but below thresholds conventionally used to distinguish an euxinic water column (Tribovillard, 2006). In the upper LO, Mo/Al values are relatively lower (min 0.36) as compared to the MO interval where values are occasionally high (max 1.43). In general, vanadium concentrations (V/Al 11.9 ± 4.4) straddle the crustal average (11.9; Rudnick, 2004), but demonstrate a trend of increasing values at the transition from the LO (8.5 ± 3.8) to the MO (12.6 ± 4.3). The same trend appears repeated within the UO (14.0 ± 3.3), where values go from below crustal average (min 5.3) to above (max 19.7). In these outcrop samples, the degree of sulphidization of iron is insignificant (Fe_{PY}/Fe_{HR} ratios on average 0.02 ± 0.02, see Supporting Information Figure S3), but much of the original sulphide was likely lost by oxidation during weathering of the outcrop. The pyrite remaining in the samples has generally high $\delta^{34}S_{Py}$ values (14.6 ‰ ±7.1) and demonstrates a trend from lower to higher values at the transition from LO to MO (Supporting Information Figure S3).

Total organic carbon (TOC) is generally low in concentration (0.6 ± 0.2 wt%) although two positive trends are notable. Firstly, a distinct gradual increase in TOC concentrations is observed at the transition between the LO and MO (from near zero to 1.1 wt%) and, then, within the base of the UO (max 1.1 wt%) (Figure 3). The isotopic composition of organic carbon ($\delta^{13}C_{org}$ −23.9 ± 0.4 ‰) demonstrates gradually more positive values from the LO (−24.3 ± 0.1 ‰) to the UO (−23.5 ± 0.2 ‰). The $\delta^{13}C_{org}$ trend shows steady overall increase of about 1 ‰, from the lowest part to the uppermost part of the 0–12 m interval (see Figure 3).

The isotopic compositions of total nitrogen ($\delta^{15}N_T$) are generally positive (1.32 ± 2.89 ‰), but show high variability (that spans over ~10 ‰ when excluding outliers, see statistical analysis below) particularly in the LO (−0.1 ± 4.4 ‰). In the MO (2.1 ± 1.9 ‰), the variability of $\delta^{15}N_T$ values decreases. In the UO (1.5 ± 1.8 ‰), smaller fluctuations are noted although variability is high.

4.3 | Statistical analyses of faunal diversity related to geochemical data

The relationship between the geochemical data that straddle rather than fall clearly above or below proxy thresholds and the faunal diversity at Sirius Passet is explored through statistical analysis. Correspondence analysis (CA) is a multivariate technique for graphically studying the relationship between two qualitative variables in a low-dimensional space and locates all the categories (or proxies) in Euclidean space. The first two dimensions of the space are plotted to investigate the associations among the categories. The technique has the advantage that measured proxies, for instance geochemical data, and individual samples are graded simultaneously and similarly

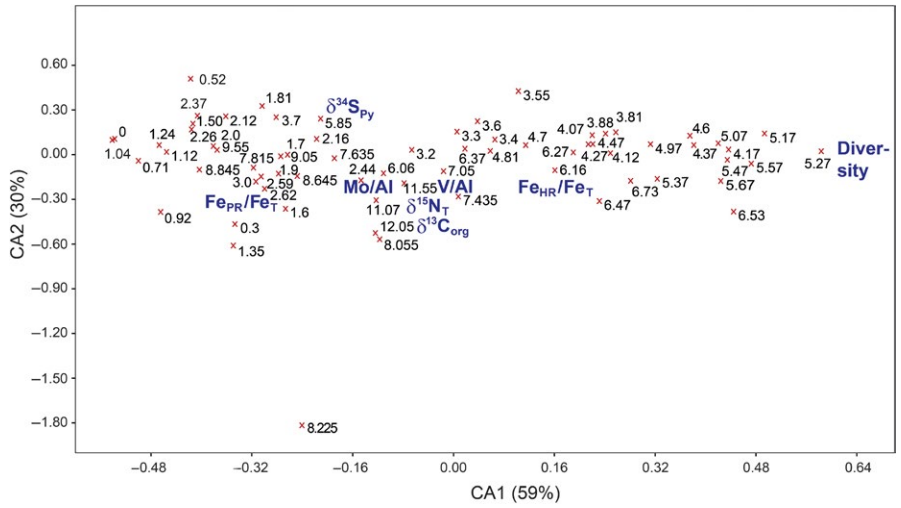

FIGURE 4 Scatter plot of correspondence analysis (CA) of the geochemical and diversity data of the fossiliferous interval (0–12 m), demonstrating that Fe_{HR}/Fe_T is placed closer to "Diversity" than the remaining geochemical proxies (each data point is depicted by its sample level). V/Al and $\delta^{15}N_T$ display a weaker, but significant, positive correlation with "Diversity." This indicates an overall similarity between Diversity and the Fe_{HR}/Fe_T, V/Al and $\delta^{15}N_T$ trends in the investigated section. Plotted numbers equal sample levels. The *x*-axis (CA1) represents 59% of the total variance and the *y*-axis (CA2) 30%. See text for explanation of correspondence analysis

scaled. As such, a scatter plot of the proxy scores (R-mode) and the sample scores (Q-mode) shows their mutual relationship. The variance is indicated along each of the CA axes (percentage). Proxies that plot close to each other typically have a related distribution. Similarly, closely spaced samples are often dominated by the same proxies.

A CA performed with PAST statistical software (Hammer, Harper, & Ryan, 2001) (Figure 4) demonstrates that faunal diversity shares a degree of similarity with the distribution of the Fe_{HR}/Fe_T ratios and, to some extent, also with the V/Al and $\delta^{15}N_T$ values. It should be noted that the $\delta^{15}N_T$ and $\delta^{13}C_{org}$ values were adjusted to produce positive values prior to CA to allow inclusion in the dataset for this type of analysis (by adding 5.28 to all $\delta^{15}N_T$ values and 24.83 to all $\delta^{13}C_{org}$ values). Notably, the samples with the highest diversity are found where Fe_{HR}/Fe_T reaches its highest values, but also V/Al, $\delta^{15}N_T$ and $\delta^{13}C_{org}$ are situated relatively close to Fe_{HR}/Fe_T in the middle part of the scatter plot (Figure 4). An additional ranking between diversity and geochemical proxies by cluster analysis, based on the Spearman's rank-order coefficient, supports the pattern displayed by the CA analysis and reveals that the distribution of Fe_{HR}/Fe_T values tracks diversity, followed by V/Al and $\delta^{15}N_T$ (Figure 5).

An overall correspondence between the data for diversity, Fe_{HR}/Fe_T, V/Al and $\delta^{15}N_T$ (seen in Figure 3) is noted and testing for statistical significance in these similarities is therefore necessary. Accordingly, the Correlation Table procedure included in the PAST software package was performed on the selected parameters using the same main outcrop dataset (Supporting Information Table S1). The Correlation Table procedure allows computation of correlation coefficients and two-tailed probabilities to show if the parameters are uncorrelated. Because some, but not all, input data are normally distributed, both a parametric (Pearson's *r*) and a non-parametric

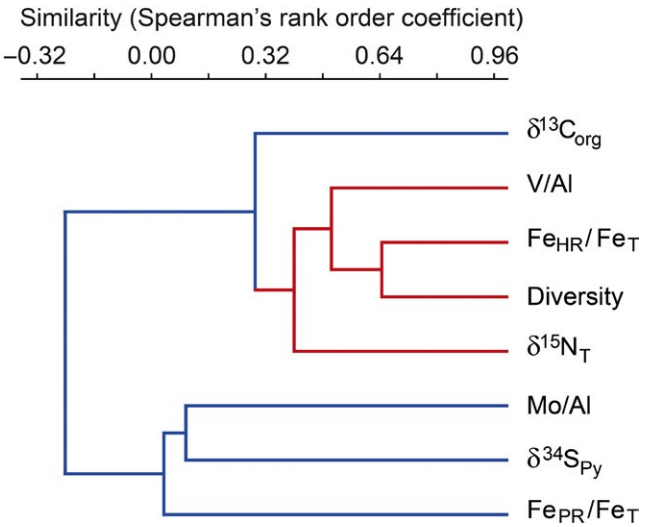

FIGURE 5 Clustering of Spearman's rank coefficients between diversity, Fe_{HR}/Fe_T, $\delta^{15}N_T$, $\delta^{34}S_{Py}$, $\delta^{13}C_{org}$ and the trace elements V/Al, and Mo/Al. Note that Fe_{HR}/Fe_T, diversity (sensu species diversity) and $\delta^{15}N_T$ are grouped closely together (marked in red). The "un-weighted pair group average" method was used for the clustering

(Kendall's tau) correlation were computed. Seven selected, geochemical proxies were tested to show if they correlate with the faunal diversity. The *p*-value (probability) for each correlation was computed to test if the null hypothesis, expressing that the correlation coefficient (Pearson's *r* or Kendall's tau) is equal to zero, is rejected. A low *p*-value (<0.05) indicates that the null hypothesis may be rejected and that the correlation is significant. The computed probability is labelled p(uncorrel) in the Supporting Information Table S1A–G. Four values considered as outliers have been omitted, viz., data associated with sample 0.16 and 0.33 (with exceptionally low $\delta^{15}N_T$ and V/Al), sample 4.9 (with exceptionally high Fe_{HR}/Fe_T), and sample 7.23 (with exceptionally high Fe_{PR} and exceptionally low V/Al).

The Correlation Table procedure performed on the bivariate faunal diversity Fe_{HR}/Fe_T dataset (Supporting Information Table S1A) shows a positive, moderate regression (Pearson's $r = 0.56$). The computed probability p(uncorrel) reveals that the correlation is clearly significant because the probability that *r* is equal to zero is far below 0.05 ($p = 5.31 \times 10^{-07}$). This supports the notion that the preserved diversity, in general, was high within the same levels where the Fe_{HR}/Fe_T ratio was also high. There is a positive, moderate to poor ($r = 0.40$) correlation between V/Al and diversity, which is significant ($p = 7.65 \times 10^{-04}$; Supporting Information Table S1B). This is also the case between $\delta^{15}N_T$ and diversity. Although the correlation in this case is poor to moderate ($r = 0.36$), the correlation is still significant ($p = 2.71 \times 10^{-03}$) (Supporting Information Table S1C). In contrast to the latter two bivariate plots, the correlation between $\delta^{13}C_{org}$ and diversity is very weak ($r = 0.14$) with an insignificant correlation ($p = 0.26$) (Supporting Information Table S1D). Also, the correlations between faunal diversity and $\delta^{34}S_{Py}$ and Mo/Al, respectively, are very weak and clearly insignificant (Supporting Information Table S1E,F). The latter three tests indicate that there is no obvious correlation of $\delta^{13}C_{org}$, $\delta^{34}S_{Py}$ and Mo/Al with the preserved faunal diversity. Interestingly, the correlation test between diversity and Fe_{PR}/Fe_T displays a significant, negative correlation, meaning that low Fe_{PR}/Fe_T values correlate with high diversities (Supporting Information Table S1G).

In summary, faunal diversity has a clearly positive correlation with the ratio of reactive iron (Fe_{HR}/Fe_T) and also, but less positively, with the vanadium enrichments (V/Al) and the isotopic composition of total nitrogen ($\delta^{15}N_T$), implying that the diversity, in general, increased when values for these three parameters rose.

5 | DISCUSSION

5.1 | Geochemical alteration

The metamorphosis of sediments at Sirius Passet could have scavenged iron oxides from the pool of highly reactive iron (Fe_{HR}) (Poulton & Canfield, 2011), complicating the application of iron-based proxies. The most immediate risk of using the proxy of Fe_{HR}/Fe_T in metamorphic rocks is that scavenged iron becomes unavailable for extraction, compromising indications of anoxic water-column chemistry. Indeed, the proxy of Fe_{HR}/FeT can be further compromised

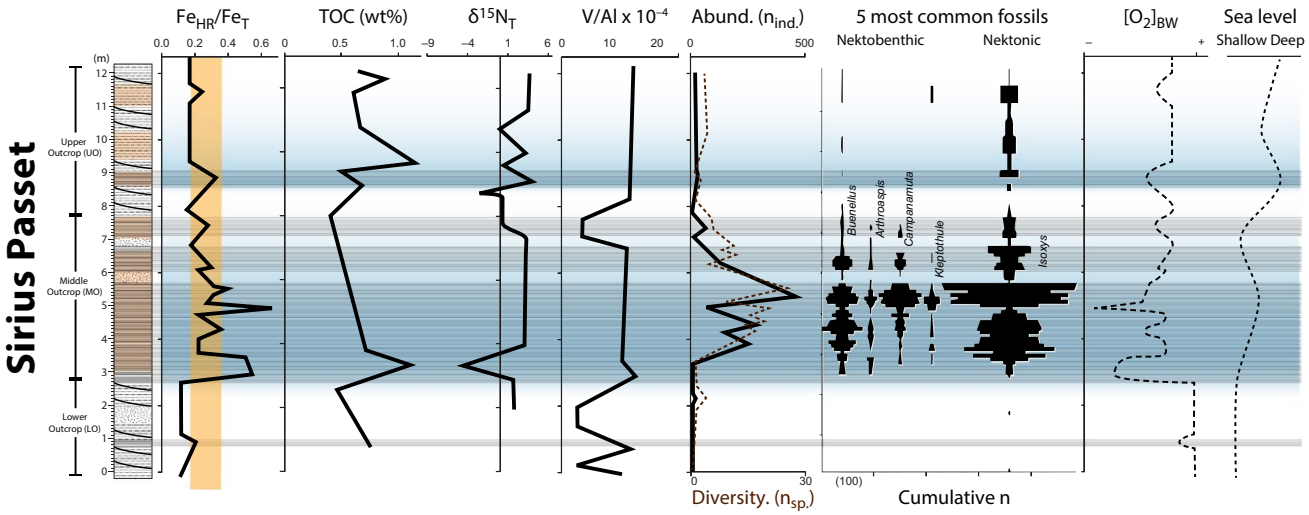

FIGURE 6 Stylized interpretation of the geochemical trends (Fe_{HR}/Fe_T, TOC, $\delta^{15}N_T$, V/Al, fossil abundance (in black) and species diversity (in dashed brown) next to cumulative abundance (n=100 between tick marks) of the five most common fossils (*Buenellus*, *Arthroaspis*, *Campanamuta*, *Kleptothule*—presumed nektobenthic—and *Isoxys*, certainly nektonic), and inferred changes (dashed black lines) of bottom water oxygen concentrations (O_{2_BW}) and relative water depth. Yellow zone brackets intermediate Fe_{HR}/Fe_T values. Proposed intervals of periodic anoxia in blue. For the stylized interpretation superimposed on geochemical data, see Supporting Information Figure S5

in outcrop samples, since weathering may oxidize and mobilize pyrite that results in an altered pool of reactive iron (Ahm, Bjerrum, & Hammarlund, 2017). For example, in the Ordovician Vinnini Creek Formation, Fe_{HR}/Fe_T is significantly lower in outcrop samples than in core samples (Ahm et al., 2017). In the present study, we have attempted to evaluate the metamorphic alteration by constructing a "*Potential* Fe_{HR}/Fe_T" ratio, based on the observation that Fe_{HR}/Fe_T and Fe_{PR}/Fe_T are inversely and well correlated ($p = 4.5 \times 10^{-11}$ $r = -0.69$, see also Supporting Information Table S1) as if some reactive iron was indeed lost into iron silicates. Although coarse and conceptual, the correction estimates a theoretical extent of remobilization and "*Potential* Fe_{HR}/Fe_T" (Figure 3) and serves to elucidate the Fe_{HR}/Fe_T at the time of deposition.

High temperatures also cause the volatilization of nitrogen and organic carbon (Bebout & Fogel, 1992), thus altering N and C concentrations and possibly isotopic compositions. For example, if ammonium, which is generally enriched in ^{14}N, is volatilized, one might expect that residual $\delta^{15}N$ and C/N values co-vary (where N values are altered, ^{14}N was lost preferentially) and, in addition, one might expect that the residual $\delta^{15}N$ has an indirect relationship with TN (where N was lost, residual $\delta^{15}N$ values are higher) (Godfrey & Falkowski, 2009). At Sirius Passet, however, trends within $\delta^{15}N$ co-vary with TN but not specifically with C/N values (Supporting Information Figure S4), arguing against metamorphic alteration of the N data. Furthermore, the metamorphic effect of volatilization would presumably affect data through the entire stratigraphy evenly. Therefore, we consider the two positive TOC excursions in the fossiliferous interval (at ~2–3 m and at 9–10 m) to reflect a primary change in carbon content and discuss them as such.

Finally, evidence of dilute sedimentary gravity flows (Strang, Armstrong, Harper, & Trabucho-Alexandre, 2016) implies some mixing of sediments and associated sediment chemistry from other sources. The mixing of sediments may have resulted, for example, in dilution of geochemical signals such as Fe_{HR}/Fe_T. Thus, the mixing of sediment during deposition, the greenschist metamorphic grade during burial and the weathering at the outcrop at Sirius Passet certainly urge caution in interpretation of the geochemical data (see also Supporting Information Appendix S1 for notes on taphonomic biases). Nevertheless, we argue that the statistical tests suggest it is reasonable to extract and interpret primary trends in the data as signals of environmental fluctuations.

5.2 | Water-column chemistry

The geochemical trends through the succession are subtle but correlated with each other, particularly at the transition from the lower (LO) to the middle (MO) outcrop, and particularly for biodiversity, Fe_{HR}/Fe_T, V/Al and $\delta^{15}N_T$. At the transition from the LO to the MO, and from medium thick to thinly laminated sediments, average Fe_{HR}/Fe_T ratios increase from 0.10 (±0.03) to 0.22 (±0.10). Within the MO, Fe_{HR}/Fe_T values are occasionally high (max 0.69), although generally below the threshold of 0.38 conventionally used to determine anoxic settings (Poulton & Canfield, 2011). On the other hand, Fe_{HR}/Fe_T values in the MO are significantly higher (see above) than the average Fe_{HR}/Fe_T ratio (0.14 ± 0.11) determined for Cambrian sediments depositing below an oxic water column (Poulton & Raiswell, 2002). The threshold of 0.38 is conservative when distinguishing anoxic from oxic water-column conditions, such that settings with anoxic or low-oxygen water-column chemistry may deposit with intermediate Fe_{HR}/Fe_T values. For example, Fe_{HR}/Fe_T ratios in the Chengjiang Lagerstätte (0.27 ± 0.08), which is roughly contemporaneous with Sirius Passet, fall below 0.38 although multiple

proxies were collectively used to infer anoxic and OMZ-like conditions (Hammarlund et al., 2017). Another example is the Ordovician Beecher's Trilobite Bed, interpreted as a dysoxic setting based on lithological and geochemical data, demonstrating Fe_{HR}/Fe_T values below 0.38 (0.33 ± 0.10) in combination with low TOC (0.4 ± 0.2) (Farrell, Briggs, Hammarlund, Sperling, & Gaines, 2013). Also, in the modern ocean, intermediate ratios of Fe_{HR}/Fe_T are observed within OMZs off Peru, from 0.16 ± 0.19 (Scholz, Severmann, McManus, Noffke et al., 2014; note slightly different definition of reactive Fe) to 0.30 ± 0.06 (Raiswell & Canfield, 1996)). Although the threshold of 0.38 is used to robustly distinguish anoxic settings from oxic, intermediate Fe_{HR}/Fe_T values (within an interval above 0.14 and below 0.38, e.g., Poulton, Fralick, & Canfield, 2010) may serve to highlight an intermediate setting. Also here, we highlight the intermediate values (see dashed lines in Figure 3) and in the MO interval at Sirius Passet, Fe_{HR}/Fe_T values fall within this "intermediate" zone. The MO interval consists of thinly laminated shale and, thus, lacks evidence of vertical bioturbation that we conventionally associate with oxic settings. On the other hand, the presence of trace-making meiofauna, constructing the network of horizontal and fine-calibre burrows within and adjacent to the carcasses of arthropods, also precludes fully anoxic conditions. Indeed, at peak Fe_{HR}/Fe_T values in the lower MO, biodiversity is low both overall (Figure 3) and within the most common nektobenthic and nektonic taxa as would be expected if the water column was predominantly anoxic (Figure 6). At the onset of the UO, Fe_{HR}/Fe_T values approach 0.38 while higher in the section only *Potential* Fe_{HR}/Fe_T values (0.29 ± 0.06) fall within the "intermediate" zone. In both the lower MO and the lower UO, peak Fe_{HR}/Fe_T values occur in conjunction with peak TOC values (max 1.1 wt%). Collectively, the iron speciation and sediment are consistent with intervals of anoxic water-column conditions in the lower MO and the lower UO but, generally, with intermediate or low-oxygen conditions in the MO.

Redox sensitive trace metals provide further clues to the water-column chemistry at the depositional location, and here, we focus on the behaviour of Mo and V. At Sirius Passet, Mo is enriched relative to the crustal average throughout our analysed section, but the enrichments are greatest in the MO (Figure 3). Vanadium is typically enriched above crustal average values in the MO and the UO, although the vanadium concentration is reduced to below crustal average values in the upper part of the LO and in the transition between the MO and the UO (Figure 3). The ratio of Al/Ti remains generally uniform throughout the section (Supporting Information Figure S8), such that a change in sediment provenance does not appear obvious and does not likely explain the trends observed in metal enrichments. We therefore regard V/Al and Mo/Al as co-enriched for most of the MO and UO, although with V/Al depletion at just before and towards the top of the MO. Co-enrichments of V and Mo (together with U) occur in sediments under anoxic water-column conditions, both in euxinic basins (Brumsack, 2006; Piper & Dean, 2002) and where the anoxic portion of OMZs overlay the sediments (Nameroff, 2002; Scholz et al., 2011). However, for sediments deposited in oxygenated waters below the anoxic core of OMZs, the behaviour of V and Mo may be somewhat variable. For example, in the oxic waters below the anoxic core of the Mexican OMZ, V loses its enrichment (and even becomes depleted) while Mo (and U) remains enriched (Nameroff, 2002). A similar trace metal fingerprint is noted in the Mesoproterozoic Xiamaling Formation, where, in addition, biomarkers for anoxygenic phototrophs established the presence of overlying anoxic waters (Zhang et al., 2016). However, off the Peruvian margin, all of the redox sensitive elements (V, Mo and U) are reduced in concentration in sediments depositing in oxygenated waters below the anoxic core of the OMZ (Boning et al., 2004; Scholz, Severmann, McManus, & Hensen, 2014), but V/Al is not reduced to the same extent as in the Mexican OMZ. Thus, we cannot be conclusive whether intervals of V/Al depletion at Sirius Passet reflect interruptions of oxygenated waters below anoxic waters, or for some other reason V/Al data (together with Fe_{HR}/Fe_T and $\delta^{15}N$ data, see Figure 5) might share statistical similarity with diversity data. Generally, though, the V and Mo enrichments support our interpretation of the Fe_{HR}/Fe_T data that the water column was anoxic or low in oxygen when animal diversity was at its highest.

Reducing water-column conditions as suggested for particularly the MO interval (see above) is accompanied by comparably higher and less variable $\delta^{15}N$ values (LO: −0.1 ± 4.4 ‰ vs MO: 2.1 ± 1.9 ‰). In the modern ocean where oxygen is low or absent, and export of organic carbon is sufficient, nitrate is partially denitrified. Denitrifying bacteria, however, preferentially utilize ^{14}N such that the residual nitrate pool available to primary producers in the surface waters becomes enriched in ^{15}N. Thus, in sediments below significant water-column denitrification, such as below modern OMZs, $\delta^{15}N$ values are elevated compared to the average oceanic mean (De Pol-Holz, Robinson, Hebbeln, Sigman, & Ulloa, 2009; Möbius, Gaye, Lahajnar, Bahlmann, & Emeis, 2011 and references therein; Ryabenko, Kock, Bange, Altabet, & Wallace, 2012). For the Cambrian Period, the oceanic mean $\delta^{15}N$ is not well constrained, so we can only consider the relative changes in ^{15}N observed at Sirius Passet. Thus, the shift to higher and less variable $\delta^{15}N$ values at Sirius Passet could have resulted from increased extents of denitrification or, alternatively, from a decline in the local importance of N_2 fixation which produces bio-available nitrogen with $\delta^{15}N$ of around 0% (Sigman et al., 2005). Although the nitrogen isotope signature at Sirius Passet is not diagnostic of denitrification, the water-column chemistry characterized by the higher and less variable $\delta^{15}N$ would in this context be consistent with nitrogenous anoxia or low-oxygen conditions.

Taken together, the Sirius Passet geochemical data are ambiguous in that they lack robust indications of both water-column anoxia, such as Fe_{HR}/Fe_T values dominantly >0.38, and well-oxygenated conditions, that would have allowed significant bioturbation. Particularly at the transition to the MO, increasing TOC and high Fe_{HR}/Fe_T values could reflect the development of water-column anoxia but, generally, the subtle behaviours of Fe_{HR}/Fe_T (particularly when evaluated as intermediate and *Potential* Fe_{HR}/Fe_T), V/Al

and Mo/Al data are consistent with low-oxygen conditions. This interpretation is supported by persistent sediment lamination that precludes a fully oxic setting and, also, horizontal burrow systems adjacent and within the carcasses of arthropods that precludes a fully anoxic water-column chemistry. The chemical fingerprint of Sirius Passet overall suggests a setting that borders between oxic and anoxic water-column chemistry.

Drivers for the development of intervals of anoxic conditions may relate to changes in sea level (affecting sedimentation rates or the position of upwelling zones), primary production (affecting carbon remineralization rates), ocean circulation (affecting oxygen replenishment) or atmospheric oxygen levels. Although sea-level change is not well-documented in the Buen Formation, an overall upward deepening trend in this part of the section is clear from the onlap pattern of basal Buen Formation quartz arenites (shallow setting) being draped by Transitional Buen mudstones (deeper setting) (Higgins et al., 1991). A trend of deepening is also consistent with the isotopic composition of organic carbon ($\delta^{13}C$), which gradually changes towards more positive values (of 0.5–1.0 ‰) through the succession, as observed in modern settings where the isotopic signal of primary production (low values) is least diluted (to higher values) by other organisms in the seaward direction (Naidu et al., 2000). While the development of anoxic conditions that intersect the depositional site may be associated with deepening, a change in primary production or sedimentation rates may also have led to increased preservation of organic carbon. Previously, it has been suggested that Sirius Passet experienced dramatic variations in climate and productivity, since preserved zircons have shapes and ages consistent with aeolian influx (Boudec et al., 2014). Therefore, the trends of increasing TOC (although generally low) at the onset of the MO and the UO (exceeding ~1 wt%) could reflect a reduction in carbon remineralization or enhanced preservation of carbon. We recognize that the question of what drove the development of anoxic conditions remains open, but changes in sea level, primary production, or both are options consistent with observations in the data.

Our interpretation of the geochemical trends within the Sirius Passet is outlined in Figure 6, where we depict how anoxic conditions intersect the seafloor twice (blue shading) and are associated with deepening (for data underlying the stylized trends, see Supporting Information Figure S5). Reducing conditions intensified at the transitions from LO to MO and from MO to UO. Our interpretation aligns with that of Boudec et al. (2014), who discussed a potential association between Cambrian Lagerstätten sites and low-oxygen settings. Our study extends the geochemical analysis of the Sirius Passet setting and concludes that it is, indeed, consistent with anoxia that developed transiently, but that low-oxygen bottom waters are generally present during its deposition.

5.3 | The paradox of in situ preservation, gravity flows and trail makers

In our Sirius Passet data, high biodiversity correlates with geochemical indicators of a low-oxygen setting (i.e., Fe_{HR}/Fe_T, Mo/Al, V/Al and $\delta^{15}N$). The correlation between reducing water-column conditions and increased biodiversity probably associates with favourable preservational conditions. For example, the low biodiversity in the LO and the UO may relate to how either water-column oxygenation or the distance to the preferred animal habitat was unfavourable for preservation (cf. Gaines, 2014). In the MO, however, as a result of a change in water-column chemistry, sea-level change or both, animals live close enough to a setting that is also facilitating better preservation. Furthermore, the correlation between reducing water-column conditions and increased biodiversity in the MO, when combined with observations of autochthonous faunal components, offers the possibility that some of the fauna actually lived within the low-oxygen setting. We must therefore consider whether some or all of the fossils were transported.

Recent studies showing the presence of sedimentary features at Sirius Passet, such as erosional bases, grading and cross-lamination (Strang, Armstrong, Harper, & Trabucho-Alexandre, 2016), suggest that dilute sediment gravity flow processes did indeed contribute to the deposition of the main outcrop rocks. These flows also appear to have been cohesive enough to have carried larger clasts and are associated with accumulations of presumably transported sponge spicules (Botting, Cárdenas, & Peel, 2015). While few trilobite specimens are disarticulated (<1%), the infauna (annelid worms) is fragmented, consistent with transport into the area from upslope locations. Sediment gravity flows at Sirius Passet may, therefore, have transported some of the fauna. On the other hand, the preservation of large and non-compressed fossils with delicate morphologies gathered on bedding planes at Sirius Passet, such as the 20 cm large nektobenthic arthropod *Arthroaspis* (cf. Budd, 1995; Stein et al., 2013) are difficult to reconcile with transport. The hypothesis that a substantial component of the fauna was not transported is further supported through three lines of observations. Firstly, we observe that the specimen of the monospecific trilobite community of *Buenellus* is predominantly orientated in life (in situ) position ("right way up"), since sedimentary features reveal the strata are inverted. This is opposite to the trilobite orientation assumed in previous accounts (Ineson & Peel, 2011), before inversion of the strata was recognized. Secondly, and in comparison with the Chengjiang fauna, the Sirius Passet biota is largely devoid of infauna or sessile benthos (Hou et al., 2017) while the arthropods, such as the large *Arthroaspis*, were part of the mobile benthos patrolling above the sediment–water interface at the depositional site. Evidence from the gut contents of the arthropods at Sirius Passet suggests that they were predators or scavengers (Peel, 2017; Strang, Armstrong, & Harper, 2016). *Arthroaspis* and its associates clearly thrived in conditions at the sediment–water interface, and their preservation is believed to have been aided by the rapid burial by sediments derived from upslope (Stein et al., 2013). Thirdly, the arthropod carapaces are characterized by a distinctive network of horizontal and shallow burrow systems, constructed by meiofauna and small macrofaunal invertebrates that lived within and adjacent to the decaying carcasses (Budd, 2011; Mángano et al., 2012). Taken together, the fauna may indeed encompass autochthonous as well as allochthonous members. These two members, furthermore, exhibit specific

characteristics. While the allochthonous members encompass fragmented worms and sponges, the autochthonous members encompass a monospecific trilobite community, together with grazers and detritivores (arthropods and halkieriids), and trace-making invertebrates that specifically mined and farmed the carcasses for nutrients.

Budd (1995) acknowledged the challenge of resolving how the soft tissues of the Sirius Passet fauna were preserved effectively in situ in an environment that hosted some trace makers and suggested that the contradictory evidence may imply that the setting "fluctuated between being capable of supporting life and being lethal" (Budd, 1995; p. 2). Since then, our understanding of animal ecosystems within low-oxygen environments has become much more refined (e.g., Sperling, Knoll, & Girguis, 2015 and references herein) and can be tested against these seemingly paradoxical observations at Sirius Passet. Although Budd's (1995) position remains valid, it is necessary to consider carefully what is considered habitable or lethal and, here, we compare the characteristics of Sirius Passet with those of modern low-oxygen environments.

5.4 | Animal life on the margins of habitability

The seemingly contradictory observations at Sirius Passet, with significant in situ animal preservation and yet the absence of bioturbation other than superficial, horizontal, small calibre burrow systems, can be understood by comparison with modern low-oxygen ecosystems. For example, in modern settings with extremely low oxygen (~0.15 ml/L), disruptive bioturbation is reduced, but nematodes and annelids thrive (Levin, 2003). In these conditions, the animals depend, to an increasing extent, on chemosynthetic nutrition (either through symbiosis or consumption of chemosynthetically fixed carbon) (Levin, 2003). The burrow systems at Sirius Passet, which are predominantly horizontal, associated with carapaces and interpreted as being used to harvest bacteria (Mángano et al., 2012), could indeed represent a source of chemosynthetic nutrition. While carapaces probably provided oases of primary nutrients in a resource-poor landscape, microbial farming within the burrows provided a secondary food source (Mángano et al., 2012). Furthermore, a monospecific trilobite community of *Elrathia kingii* in the Cambrian Wheeler Shale has been associated with extreme low-oxygen conditions and a pioneering strategy (Gaines & Droser, 2003). Thus, it is feasible that the monospecific community of *Buenellus higginsi* also represents pioneers at the boundary zones of anoxic and dysoxic bottom waters that was autochthonously preserved. Thus, the lack of extensive bioturbation, but the presence of the trace makers, pioneering species, and chemosynthesis-based nutrition, may be reconciled with extremely low-oxygen settings. Figure 7 presents an overview that captures the observations at Sirius Passet mapped onto the boundaries between anoxic, OMZ-like, and oxic conditions.

We cannot directly evaluate oxygen concentrations at Sirius Passet, but we can extend the comparison between its setting and ecology to those of modern OMZs (defined as oxygen concentrations <0.5 ml/L, Levin, 2003). Modern OMZ communities commonly include sponges, polychaetes and crustaceans, but rarely echinoderms or molluscs (Levin, 2003). The OMZ communities are generally low in diversity and their ecology follows some overall patterns. For example, sponges and arthropods are located at the fringes of the OMZs (at O_2 concentrations around 0.20 ml/L) and diversity decreases at concentrations below 0.15 ml/L (Levin, 2003). Within the OMZs (at O_2 concentrations of 0.16 ml/L), observations include reduced bioturbation, chemosynthesis-based nutrition, and of high density and low diversity communities of, for example, annelids (Levin, 2003). The modern OMZ pelagic communities are characterized by, for example, large predators and detritivores, such as the vampire squid (found at 0.4 ml/L; Hoving & Robison, 2012), and a short food chain (Levin, 2003; and references therein). In comparison, the Sirius Passet fauna is generally also of low diversity; arthropods and worms (annelids and nematodes) are common (Conway Morris, Peel, Higgins, Soper, & Davis, 1987), while echinoderms and molluscs are (Budd, 1995; Vinther & Nielsen, 2005). Additionally, the Sirius Passet fauna is dominated by presumed predatory nektobenthic arthropods with some detritivores and scavengers, and the food chain appears short. Thus, some ecological characteristics are shared between the modern OMZ and the Sirius Passet biota.

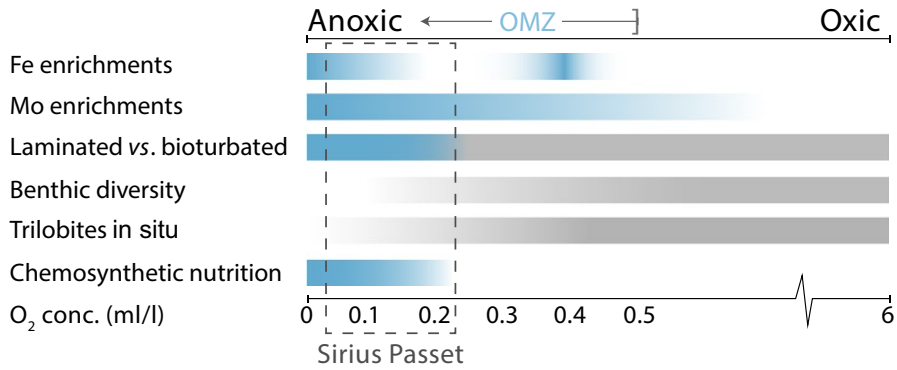

FIGURE 7 Water-column chemistry (from anoxic to oxic) inferred from chemical and ecological characteristics (for references see Discussion), where observations from the Sirius Passet main outcrop (grey dashed box) bracket its setting as significantly low in oxygen. Oxygen concentrations are suggestive and based on comparison with modern OMZ settings where, particularly, bioturbation is observed to be reduced at 0.2 ml/L (Levin, 2003)

If the Sirius Passet fauna is analogous to modern OMZ faunas, there are parallels to be drawn with regard to oxygen concentrations. Since the laminated sediments of the main outcrop suggest insignificant bioturbation, oxygen concentrations could be presumed to have been around 0.15 ml/L (Levin, 2003). In turn, the Sirius Passet arthropods may have lived at oxygen concentrations as low as 0.15–0.20 (near the sediment) or at ~0.4 ml/L (in the water column). Such low-oxygen concentrations (0.2–0.4 ml/L) today would represent a dramatic depletion (94–96%) from fully saturated surface waters at ~6 ml/L. However, under a Cambrian atmosphere with an estimated O_2 of <20%PAL (Lenton et al., 2016), the same concentrations would only require 66–83% depletion, hence a less extreme and more easily achieved exhaustion.

Taken together, we interpret the Sirius Passet data to indicate a dynamic setting, capturing turbulence (initiating sediment gravity flows and quieter background sedimentation) together with low and fluctuating oxygen concentrations. Geochemical data and palaeontological data, when compared to modern OMZs (e.g., chemosynthetic nutrition, monospecific pioneering trilobite community, short food chain, the characteristics of autochthonous and allochthonous faunal members), collectively, are also consistent with an interpretation that extremely low-oxygen concentrations restricted bioturbation but not the establishment of a largely nektobenthic community. While optimal conditions for preservation likely associate with fluctuations in water-column chemistry and sea level, we envisage that much of the Sirius Passet animal community also lived at the site during conditions of extremely low water-column oxygen concentrations.

Our interpretation of the data postulates that the Sirius Passet Lagerstätte represents an early Cambrian biota that, in terms of oxygen, lived at the margins of its tolerance. The development of such a marginal, low-oxygen setting is analogous to evidence of chemical water-column stratification, and variability, on the Yangtze platform containing the age-equivalent Chengjiang fauna (Och & Shields-Zhou, 2012). The Yangtze platform hosts contemporaneous evidence of extensive euxinia (Cremonese et al., 2013; Wen et al., 2015), ferruginous (Canfield et al., 2008; Feng et al., 2014) and OMZ-like conditions (Hammarlund et al., 2017; Wen et al., 2015), as well as presumed oxygenation (Cremonese et al., 2013) of the water column. Thus, the vastly distant continental platforms in the early Cambrian now both demonstrate chemically variable settings, prone to anoxia or low-oxygen conditions. Now, if early animal biotas were established at the margins of (what we today perceive as) habitability, we must reasonably ask to what extent low-oxygen conditions or the interplay between habitable and inhospitable chemistry dictated ecological patterns and provided evolutionary selective pressure during the Cambrian Explosion?

ACKNOWLEDGMENTS

The authors wish to acknowledge funding from Agouron Institute, Carlsberg Foundation, Danish National Research Foundation (DNRF53), the Villum Foundation (grant 16518) and Geocenter Denmark. DATH thanks the Leverhulme Trust and the Wenner-Gren Foundation for additional support. We thank Jakob Walløe Hansen for assisting with field work in the high Arctic. We also thank Heidi Grøn Jensen, Dina Holmgaard Skov and Mette Andersen for invaluable assistance, and the reviewers for much appreciated input and comments. The authors declare no conflict of interests.

ORCID

Emma U. Hammarlund http://orcid.org/0000-0001-7625-4793
M. Paul Smith http://orcid.org/0000-0002-5141-1577
Donald E. Canfield http://orcid.org/0000-0001-7602-8366

REFERENCES

Ahm, A.-S. C., Bjerrum, C. J., & Hammarlund, E. U. (2017). Disentangling the record of diagenesis, local redox conditions, and global seawater chemistry during the latest Ordovician glaciation. *Earth and Planetary Science Letters*, *459*, 145–156. https://doi.org/10.1016/j.epsl.2016.09.049

Bebout, G. E., & Fogel, M. L. (1992). Nitrogen-isotope compositions of metasedimentary rocks in the Catalina Schist, California: Implications for metamorphic devolatilization history. *Geochimica Cosmochimica Acta*, *56*(7), 2839–2849. https://doi.org/10.1016/0016-7037(92)90363-N

Boning, P., Brumsack, H. J., Bottcher, M. E., Schnetger, B., Kriete, C., Kallmeyer, J., & Borchers, S. L. (2004). Geochemistry of Peruvian near-surface sediments. *Geochimica et Cosmochimica Acta*, *68*(21), 4429–4451. https://doi.org/10.1016/j.gca.2004.04.027

Botting, J. P., Cárdenas, P., & Peel, J. S. (2015). A crown-group demosponge from the early Cambrian Sirius Passet Biota, North Greenland. *Palaeontology*, *58*(1), 35–43. https://doi.org/10.1111/pala.12133

Boudec, A. L., Ineson, J., Rosing, M., Døssing, L., Martineau, F., Lécuyer, C., & Albarède, F. (2014). Geochemistry of the Cambrian Sirius Passet Lagerstätte, Northern Greenland. *Geochemistry, Geophysics, Geosystems*, *15*(4), 886–904. https://doi.org/10.1002/2013GC005068

Brumsack, H. J. (2006). The trace metal content of recent organic carbon-rich sediments: Implications for Cretaceous black shale formation. *Palaeogeography Palaeoclimatology Palaeoecology*, *232*(2–4), 344–361. https://doi.org/10.1016/j.palaeo.2005.05.011

Budd, G. E. (1995). *Kleptothule rasmusseni* gen. et sp. nov.: An? olenellinid-like trilobite from the Sirius Passet fauna (Buen Formation, Lower Cambrian, North Greenland). *Transactions of the Royal Society of Edinburgh: Earth Sciences*, *86*(01), 1–12.

Budd, G. E. (2011). *Campanamuta mantonae* gen. et. sp. nov., an exceptionally preserved arthropod from the Sirius Passet Fauna (Buen Formation, lower Cambrian, North Greenland). *Journal of Systematic Palaeontology*, *9*(2), 217–260. https://doi.org/10.1080/14772019.2010.492644

Butterfield, N. J. (1995). Secular distribution of Burgess-Shale-type preservation. *Lethaia*, *28*, 1–13. https://doi.org/10.1111/j.1502-3931.1995.tb01587.x

Canfield, D. E. (1989). Sulfate reduction and oxic respiration in marine sediments: Implications for organic carbon preservation in euxinic environments. *Deep-Sea Research*, *36*, 121–138. https://doi.org/10.1016/0198-0149(89)90022-8

Canfield, D. E., Poulton, S. W., Knoll, A. H., Narbonne, G. M., Ross, G., Goldberg, T., & Strauss, H. (2008). Ferruginous conditions dominated later Neoproterozoic deep water chemistry. *Science*, *321*, 949–952. https://doi.org/10.1126/science.1154499

Chen, X., Ling, H.-F., Vance, D., Shields-Zhou, G. A., Zhu, M., Poulton, S. W., … Archer, C. (2015). Rise to modern levels of ocean oxygenation coincided with the Cambrian radiation of animals. *Nature Communications*, *6*, 7142.

Cocks, L. R. M., & Torsvik, T. H. (2002). Earth geography from 500 to 400 million years ago: A faunal and palaeomagnetic review. *Journal of the Geological Society*, *159*, 631–644.

Cohen, K., Finney, S., Gibbard, P., & Fan, J.-X. (2013). The ICS international chronostratigraphic chart. *Episodes*, *36*(3), 199–204.

Conway Morris, S. (1989). Early metazoans. *Science Progress*, *Oxford*, *73*, 81–99.

Conway Morris, S., & Peel, J. (1995). Articulated halkieriids from the Lower Cambrian of North Greenland and their role in early protostome evolution. *Philosophical Transactions: Biological Sciences*, *347*, 305–358. https://doi.org/10.1098/rstb.1995.0029

Conway Morris, S., Peel, J., Higgins, A., Soper, N., & Davis, N. (1987). A Burgess shale-like fauna from the Lower Cambrian of North Greenland. *Nature*, *326*, 181–183. https://doi.org/10.1038/326181a0

Cremonese, L., Shields-Zhou, G., Struck, U., Ling, H.-F., Och, L., Chen, X., & Li, D. (2013). Marine biogeochemical cycling during the early Cambrian constrained by a nitrogen and organic carbon isotope study of the Xiaotan section, South China. *Precambrian Research*, *225*, 148–165. https://doi.org/10.1016/j.precamres.2011.12.004

Dahl, T. W., Ruhl, M., Hammarlund, E. U., Canfield, D. E., Rosing, M. T., & Bjerrum, C. J. (2013). Tracing euxinia by molybdenum concentrations in sediments using handheld X-ray fluorescence spectroscopy (HHXRF). *Chemical geology*, *360–361*, 241–251. https://doi.org/10.1016/j.chemgeo.2013.10.022

De Pol-Holz, R., Robinson, R. S., Hebbeln, D., Sigman, D. M., & Ulloa, O. (2009). Controls on sedimentary nitrogen isotopes along the Chile margin. *Deep-Sea Research Part II-Topical Studies in Oceanography*, *56*(16), 1100–1112.

Farrell, Ú. C., Briggs, D. E., Hammarlund, E. U., Sperling, E. A., & Gaines, R. R. (2013). Paleoredox and pyritization of soft-bodied fossils in the Ordovician Frankfort Shale of New York. *American Journal of Science*, *313*(5), 452–489. https://doi.org/10.2475/05.2013.02

Feng, L., Li, C., Huang, J., Chang, H., & Chu, X. (2014). A sulfate control on marine mid-depth euxinia on the early Cambrian (ca. 529–521 Ma) Yangtze platform, South China. *Precambrian Research*, *246*, 123–133. https://doi.org/10.1016/j.precamres.2014.03.002

Gaines, R. (2014). Burgess shale-type preservation and its distribution in space and time. *The Paleontological Society Papers*, *20*, 123–146. https://doi.org/10.1017/S1089332600002837

Gaines, R. R., & Droser, M. L. (2003). Paleoecology of the familiar trilobite *Elrathia kingii*: An early exaerobic zone inhabitant. *Geology*, *31*(11), 941–944. https://doi.org/10.1130/G19926.1

Godfrey, L., & Falkowski, P. G. (2009). The cycling and redox state of nitrogen in the Archaean ocean. *Nature Geoscience*, *2*(10), 725–729. https://doi.org/10.1038/ngeo633

Hammarlund, E. U., Gaines, R. R., Prokopenko, M. G., Qi, C., Hou, X.-G., & Canfield, D. E. (2017). Early Cambrian oxygen minimum zone-like conditions at Chengjiang. *Earth and Planetary Science Letters*, *475*, 160–168. https://doi.org/10.1016/j.epsl.2017.06.054

Hammer, Ø., Harper, D. A. T., & Ryan, P. D. (2001). PAST: Paleontological statistics software package for education and data analysis. *Palaeontologia Electronica*, *4*(1), 1–9.

Higgins, A., Ineson, J., Peel, J., Surlyk, F., & Sønderholm, M. (1991). Lower palaeozoic franklinian basin of North Greenland. *Bull Grønlands geol Unders*, *160*, 71–139.

Hou, X.-G., Siveter, D. J., Siveter, D. J., Aldridge, R. J., Cong, P.-Y., Gabbott, S. E., … Williams, M. (2017). *The evolutionary significance of the chengjiang biota*, *The Cambrian Fossils of Chengjiang*, *China* (pp. 7–11). Chichester, West Sussex, UK: John Wiley & Sons Ltd.. https://doi.org/10.1002/9781118896372

Hoving, H. J. T., & Robison, B. H. (2012). Vampire squid: Detritivores in the oxygen minimum zone. *Proceedings of the Royal Society B: Biological Sciences*, *279*, 4559–4567. https://doi.org/10.1098/rspb.2012.1357

Ineson, J. R., & Peel, J. S. (2011). Geological and depositional setting of the Sirius Passet Lagerstätte (Early Cambrian), North Greenland. *Canadian Journal of Earth Sciences*, *48*(8), 1259–1281. https://doi.org/10.1139/e11-018

Ivantsov, A. Y., Zhuravlev, A. Y., Leguta, A. V., Krassilov, V. A., Melnikova, L. M., & Ushatinskaya, G. T. (2005). Palaeoecology of the early Cambrian Sinsk biota from the Siberian platform. *Palaeogeography*, *Palaeoclimatology*, *Palaeoecology*, *220*(1), 69–88. https://doi.org/10.1016/j.palaeo.2004.01.022

Knoll, A. H., & Carroll, S. B. (1999). Early animal evolution: Emerging views from comparative biology and geology. *Science*, *184*, 2129–2137. https://doi.org/10.1126/science.284.5423.2129

Kristensen, E., Penha-Lopes, G., Delefosse, M., Valdemarsen, T., Quintana, C. O., & Banta, G. T. (2012). What is bioturbation? The need for a precise definition for fauna in aquatic sciences *Marine Ecology Progress Series*, *446*, 285–302. https://doi.org/10.3354/meps09506

Legg, D., & Vannier, J. (2013). The affinities of the cosmopolitan arthropod *Isoxys* and its implications for the origin of arthropods. *Lethaia*, *46*, 540–550. https://doi.org/10.1111/let.12032

Lenton, T. M., Dahl, T. W., Daines, S. J., Mills, B. J. W., Ozaki, K., Saltzman, M. R., & Porada, P. (2016). Earliest land plants created modern levels of atmospheric oxygen. *Proceedings of the National Academy of Sciences*, *113*(35), 9704–9709. https://doi.org/10.1073/pnas.1604787113

Levin, L. (2003). Oxygen minimum zone benthos: Adaptation and community response to hypoxia. *Oceanography and Marine Biology Annual Review*, *41*, 1–45.

Lyons, T. W., & Severmann, S. (2006). A critical look at iron paleoredox proxies: New insights from modern euxinic marine basins. *Geochimica et Cosmochimica Acta*, *70*(23), 5698–5722. https://doi.org/10.1016/j.gca.2006.08.021

Mángano, M. G., Bromley, R. G., Harper, D. A. T., Nielsen, A. T., Smith, M. P., & Vinther, J. (2012). Nonbiomineralized carapaces in Cambrian seafloor landscapes (Sirius Passet, Greenland): Opening a new window into early Phanerozoic benthic ecology. *Geology*, *40*(6), 519–522. https://doi.org/10.1130/G32853.1

Möbius, J., Gaye, B., Lahajnar, N., Bahlmann, E., & Emeis, K. C. (2011). Influence of diagenesis on sedimentary $\delta^{15}N$ in the Arabian Sea over the last 130kyr. *Marine Geology*, *284*(1), 127–138.

Naidu, A. S., Cooper, L. W., Finney, B. P., Macdonald, R. W., Alexander, C., & Semiletov, I. P. (2000). Organic carbon isotope ratios (δ13C) of Arctic Amerasian Continental shelf sediments. *International Journal of Earth Sciences*, *89*(3), 522–532. https://doi.org/10.1007/s005310000121

Nameroff, T. J. (2002). Suboxic trace metal geochemistry in the eastern tropical North Pacific. *Geochimica Et Cosmochimica Acta*, *66*(7), 1139–1158. https://doi.org/10.1016/S0016-7037(01)00843-2

Nielsen, M. L., Rasmussen, J. A., & Harper, D. A. T. (2017). Sexual dimorphism within the stem-group arthropod *Isoxys volucris* from the Sirius Passet Lagerstätte, North Greenland. *Bulletin of the Geological Society of Denmark*, *65*, 47–58.

Och, L. M., & Shields-Zhou, G. A. (2012). The Neoproterozoic oxygenation event: Environmental perturbations and biogeochemical cycling. *Earth-Science Reviews*, *110*(1), 26–57. https://doi.org/10.1016/j.earscirev.2011.09.004

Peel, J. S. (2010). A corset-like fossil from the *Cambrian* Sirius Passet Lagerstätte of North Greenland and its implications for cycloneuralian evolution. *Journal of Paleontology*, *84*(2), 332–340. https://doi.org/10.1666/09-102R.1

Peel, J. S. (2017). Mineralized gutfills from the Sirius Passet Lagerstätte (Cambrian Series 2) of North Greenland. *GFF*, *139*(2), 83–91. https://doi.org/10.1080/11035897.2016.1260051

Piper, D. Z., & Dean, W. E. (2002). *Trace-element deposition in the Cariaco Basin, Venezuela shelf, under sulfate-reducing conditions-a history of the local hydrography and global climate, 20 Ka to the present: U.S. Geological Survey*. 1670.

Poulton, S. W., & Canfield, D. E. (2005). Development of a sequential extraction procedure for iron: implications for iron partitioning in continentally-derived particulates. *Chemical Geology*, *214*, 209–221. https://doi.org/10.1016/j.chemgeo.2004.09.003

Poulton, S. W., & Canfield, D. E. (2011). Ferruginous Conditions: A Dominant Feature of the Ocean through Earth's History. *Elements*, *7*(2), 107–112. https://doi.org/10.2113/gselements.7.2.107

Poulton, S. W., Fralick, P. W., & Canfield, D. E. (2010). Spatial variability in oceanic redox structure 1.8 billion years ago. *Nature Geoscience*, *3*(7), 486–490. https://doi.org/10.1038/ngeo889

Poulton, S. W., & Raiswell, R. (2002). The low-temperature geochemical cycle of iron: From continental fluxes to marine sediment deposition. *American Journal of Science*, *302*, 774–805. https://doi.org/10.2475/ajs.302.9.774

Raiswell, R., & Canfield, D. E. (1996). Rates of reaction between silicate iron and dissolved sulfide in Peru Margin sediments. *Geochimica et Cosmochimica Acta*, *60*, 2777–2787. https://doi.org/10.1016/0016-7037(96)00141-X

Raiswell, R., & Canfield, D. E. (1998). Sources of iron for pyrite formation in marine sediments. *American Journal of Science*, *298*, 219–245. https://doi.org/10.2475/ajs.298.3.219

Rudnick, R. L. (2004). Composition of the continental crust. In R. L. Rudnick (Ed.), *Treatise on geochemistry: The crust*, Vol. *3* (pp. 1–64). Amsterdam, the Netherlands: Elsevier.

Ryabenko, E., Kock, A., Bange, H. W., Altabet, M. A., & Wallace, D. W. R. (2012). Contrasting biogeochemistry of nitrogen in the Atlantic and Pacific Oxygen Minimum Zones. *Biogeosciences*, *9*(1), 203–215.

Scholz, F., Hensen, C., Noffke, A., Rohde, A., Liebetrau, V., & Wallmann, K. (2011). Early diagenesis of redox-sensitive trace metals in the Peru upwelling area - response to ENSO-related oxygen fluctuations in the water column. *Geochimica et Cosmochimica Acta*, *75*, 7257–7276. https://doi.org/10.1016/j.gca.2011.08.007

Scholz, F., Severmann, S., McManus, J., & Hensen, C. (2014). Beyond the Black Sea paradigm: The sedimentary fingerprint of an open-marine iron shuttle. *Geochimica et Cosmochimica Acta*, *127*, 368–380. https://doi.org/10.1016/j.gca.2013.11.041

Scholz, F., Severmann, S., McManus, J., Noffke, A., Lomnitz, U., & Hensen, C. (2014). On the isotope composition of reactive iron in marine sediments: Redox shuttle versus early diagenesis. *Chemical Geology*, *389*, 48–59. https://doi.org/10.1016/j.chemgeo.2014.09.009

Sigman, D. M., Granger, J., DiFiore, P. J., Lehmann, M. M., Ho, R., Cane, G., & van Geen, A. (2005). Coupled nitrogen and oxygen isotope measurements of nitrate along the eastern North Pacific margin. *Global Biogeochemical Cycles*, *19*(4), GB4022.

Sperling, E. A., Knoll, A. H., & Girguis, P. R. (2015). The ecological physiology of earth's second oxygen revolution. *Annual Review of Ecology, Evolution, and Systematics*, *46*(1), 215–235. https://doi.org/10.1146/annurev-ecolsys-110512-135808

Stein, M., Budd, G. E., Peel, J. S., & Harper, D. A. T. (2013). *Arthroaspis* n. gen., a common element of the Sirius Passet Lagerstätte (Cambrian, North Greenland), sheds light on trilobite ancestry. *BMC evolutionary Biology*, *13*(1), 1.

Stein, M., Peel, J. S., Siveter, D. J., & Williams, M. (2010). *Isoxys* (Arthropoda) with preserved soft anatomy from the Sirius Passet Lagerstätte, lower Cambrian of North Greenland. *Lethaia*, *43*(2), 258–265.

Strang, K. M., Armstrong, H. A., & Harper, D. A. T. (2016). Minerals in the gut: Scoping a Cambrian digestive system: Royal Society Open. *Science*, *3*(11).

Strang, K., Armstrong, H. A., Harper, D. A. T., & Trabucho-Alexandre, J. (2016). The Sirius Passet Lagerstätte: silica death masking opens the window on the earliest matground community of the Cambrian Explosion. *Lethaia*, *49*(4), 631–643. https://doi.org/10.1111/let.12174

Topper, T. P., Greco, F., Hofmann, A., Beeby, A., & Harper, D. A. T. (2018). Characterization of kerogenous films and taphonomic modes of the Sirius Passet Lagerstätte, Greenland. *Geology*, *46*, 359–362. https://doi.org/10.1130/G39930.1

Torsvik, T. H. (2009). *BugPlates: Linking biogeography and palaeogeography*. Retrieved from http://www.geodynamics.no

Tribovillard, N. (2006). Trace metals as paleoredox and paleoproductivity proxies: An update. *Chemical Geology*, *232*, 12–32. https://doi.org/10.1016/j.chemgeo.2006.02.012

Vidal, G., & Peel, J. S. (1993). *Acritarchs from the Lower Cambrian Buen Formation in North Greenland*: Bull./Gronlands geol. undersogelse.

Vinther, J., & Nielsen, C. (2005). The early Cambrian Halkieria is a mollusc. *Zoologica Scripta*, *34*(1), 81–89. https://doi.org/10.1111/j.1463-6409.2005.00177.x

Vinther, J., Smith, M. P., & Harper, D. A. T. (2011). Vetulicolians from the Lower Cambrian Sirius Passet Lagerstätte, North Greenland, and the polarity of morphological characters in basal deuterostomes. *Palaeontology*, *54*(3), 711–719. https://doi.org/10.1111/j.1475-4983.2011.01034.x

Wen, H., Fan, H., Zhang, Y., Cloquet, C., & Carignan, J. (2015). Reconstruction of early Cambrian ocean chemistry from Mo isotopes. *Geochimica et Cosmochimica Acta*, *164*, 1–16. https://doi.org/10.1016/j.gca.2015.05.008

Williams, M., Siveter, D. J., & Peel, J. S. (1996). *Isoxys* (Arthropoda) from the Early Cambrian Sirius Passet Lagerstätte, North Greenland. *Journal of Paleontology*, *70*(6), 947–954. https://doi.org/10.1017/S0022336000038646

Zhang, S., Wang, X., Wang, H., Bjerrum, C. J., Hammarlund, E. U., Costa, M. M., … Canfield, D. E. (2016). Sufficient oxygen for animal respiration 1,400 million years ago. *Proceedings of the National Academy of Sciences*, *113*(7), 1731–1736. https://doi.org/10.1073/pnas.1523449113

SUPPORTING INFORMATION

Additional supporting information may be found online in the Supporting Information section at the end of the article.

How to cite this article: Hammarlund EU, Smith MP, Rasmussen JA, Nielsen AT, Canfield DE, Harper DAT. The Sirius Passet Lagerstätte of North Greenland—A geochemical window on early Cambrian low-oxygen environments and ecosystems. *Geobiology*. 2018;00:1–15. https://doi.org/10.1111/gbi.12315